Solid Freeform Fabrication 2016: Proceedings of the 27th Annual International Solid Freeform Fabrication Symposium – An Additive Manufacturing Conference
Reviewed Paper

RESEARCH UPDATES ON THE ADDITIVE MANUFACTURING OF NICKEL BASED SUPERALLOYS

Sankaranarayanan Seetharaman, Manickavasagam Krishnan,
Francis Goh Chung Wen, Niaz Ahmed Khan and Gary Ng Ka Lai

Advanced Remanufacturing and Technology Centre,
Agency for Science, Technology and Research, CleanTech Two, Singapore 637143

Abstract

Over the last decade, additive manufacturing technology has consistently evolved as a sophisticated rapid manufacturing tool that allows direct fabrication of an end-usable part without extensive tooling. The methodology of layer-by-layer fabrication demonstrates the novel prospects of fabricating complex and multifunctional components and the aerospace and automotive industries have been quite successful in adopting various additive technologies for the use in jet engines, power plants and reactor vessels. This article will systematically review the properties of nickel-based superalloys using different additive manufacturing methods. In the first section, the types of additive manufacturing methods are briefly introduced. The properties of Ni superalloy powders and the characterization methods are then discussed. The mechanical properties displayed by additively manufactured Ni superalloys are presented and discussed based on the influence of different processing and post-processing variables.

Key Words: Additive Manufacturing, Nickel superalloys, Powder Metallurgy, Microstructure, Mechanical properties, Surface Finish

Additive Manufacturing Technology Landscape

Additive manufacturing processes refer to layer by layer joining of powder materials to make end-usable products. The benefits of AM over traditional manufacturing include (i) complex part manufacturing without excess tooling needs, (ii) reduced number of processing steps and (iii) minimal requirement for post-processing[1].

While all AM processes involve layer-based generic approach starting from CAD model generation to post-processing/finishing of built parts, they essentially differ in the processing strategy by means of (i) the materials that can be used and their initial properties, (ii) how the layers are created, and (iii) how the layers are bonded to each other. Such differences will eventually determine the accuracy of build part, its properties and performance [1,2].

The commercial AM processes are broadly classified into three main groups: (i) liquid-based systems, (ii) solid-based systems and (iii) powder-based systems [3,4]. While the liquid-based systems are effective for polymer processing, powder and solid-based systems can be utilized for fabricating metallic materials.

Solid based systems

Fused deposition modeling (FDM), ultrasonic consolidation (UC) and electron beam additive manufacturing (EBAM) processes use solid raw material to produce three-dimensional solid objects. While the FDM process commercialized by Stratasys typically produces polymer 3D solid parts by extruding the thermoplastic material through a nozzle, UC patented by Solidica and Sciaky's EBAM techniques can be employed for metallic parts fabrication.

UC process produce complex part geometries by sequentially laminating the metal foil layers using an ultrasonic sonotrode to induce vibrations for joining/welding. Unlike other additive technologies wherein the bonding between layers is generated by selective heating/melting of powder materials, UC applies ultrasonic joining technique to produce true metallurgical bonds between layers of metallic materials. This method can be successfully used to manufacture low melting point metal parts with following advantages: (i) higher fabrication speed, (ii) no requirement of control atmosphere, and (iii) reduced residual stresses and part distortion.

EBAM uses wire feed raw material for fabricating metallic materials. This method promises high deposition rates and ability to fabricate large part sizes. A similar electron beam freeform fabrication (EBF^3) method has been used by NASA to build parts in zero gravity environments [5,6].

Powder based systems

Nowadays, there is an enormous interest on the powder-based AM systems based on laser and electron beam source to fabricate metallic parts and components. Figure 1a shows the family tree and applicability of different powder bed AM systems. The general illustration of an AM powder bed system is presented in Figure 1b.

Binder Jetting involves layer by layer spreading of powder materials which were subsequently joined by selectively applying glue using an inkjet head. The major advantage of this method is that it can be applied for joining metal powders. The major limitation of this process is that it always requires post processing steps such as oven sintering, isostatic pressing etc., as the final product from this process is not very strong.

Laser sintering (LS) process was first developed at the University of Texas. This process involves layer by layer spreading of powder and subsequent sintering using a low power (CO_2) laser source. The general processing procedure includes a roller to deposit a fine layer of powder on the build platform. The laser source (typically 50W) will then selectively sinter the powder and completes the fabrication of one layer. For the next layer, the powder bed is then lowered by one layer thickness and the new layer of powder material is then deposited and sintered. This process is continued until the complete part is produced. As the power of the laser in the SLS machine is not enough to melt metals and ceramics, they are often coated with the polymer which acts as a binder. After sintering, the binder is removed (by burning) and then the mold is infiltrated with a low melting point metal or alloy.

Figure 1 (a) Family Tree & (b) Illustration of Powder Bed AM Systems

Laser Melting (LM) is very similar to sintering process, except that a high power (fiber) laser source is used to selectively melt the uncoated metal powders melted to produce high-strength

metallic parts. This method shows better suitability to produce full dense parts approaching 99.9% density in a direct way, without post-infiltration, sintering or HIP. Since the SLM process does not require burning out of polymer and post-densification, the time required for producing a metal part is reduced in SLM when compared to the SLS process. Another major advantage lies in its high feasibility in processing non-ferrous metals such as Ti, Al, Cu, which cannot be well processed using partial melting, and associated high viscosity and balling phenomenon. However, the high energy level required for melting the powder materials and the risk of unstable melt pool resulting in large shrinkage and residual stress are regarded as key limitations. Currently, the LM machines are marketed by 3D systems, Concept laser, EOS, MTT and Phenix.

Laser deposition methods involve localized melting and deposition of powder materials using a high power laser source. The carrier medium which is usually an inert gas feeds the powder through nozzles. Upon interaction with laser, the powder melts and the molten material is deposited on the platform based on the CAD data. This technology has been commercialized by POM, Optomec, Aeromet and MTS as direct metal deposition (DMD), laser engineered net shaping (LENS), laser rapid forming (DRF), laser cladding (LC), and laser additive manufacturing (LAM) respectively. The deposition methods can be effectively used to produce titanium alloys, nickel alloys, steels, cobalt alloys, alumnum alloys and composite coatings. Their advantages include (i) production of fully dense materials with good metallurgical properties at reasonable speeds, (ii) capability to build intricate features and shapes, (iii) ability to integrate features to cast or forged parts for repair purposes. The major limitations are (i) difficulty in building overhung parts and features, (ii) microstructural control, (iii) poor surface finish, and (iv) residual stress.

Electron beam melting (EBM) process developed at Chalmers University of Technology, Sweden and marketed by Arcam, works on the similar principle as selective laser melting except that the melting of powder materials was done using a focused electron beam emitted from a heated tungsten filament. The electron beam interacts with the metal powder on the platform so that the kinetic energy of the electron beam is converted to heat and melts the region of the metal powder. Since this process requires high vacuum for electron beam processing, better mechanical properties can be achieved by using EBM process. However, the EBM process has few limitations such as (i) process stability, (ii) part defects, (iii) quality variations, and (iv) size of the building chamber.

Although there have been only a limited number of commercial alloys that can be used in AM processes, the aerospace and automotive industries are fairly successful in adopting additively processed nickel-based superalloys for applications in gas turbines, heat exchangers, reactor vessels, etc.[7]. Available open literature indicates that the AM processes develop a fine-grained, oriented microstructure in the Ni-based superalloys resulting in excellent mechanical properties that are comparable and superior to that of other conventional fabrication methods [8,9]. However, the mechanical anisotropy, residual stress and poor surface finish resulting from AM processes need to be controlled by optimizing the (i) initial powder properties, (ii) processing conditions and process variables, and (iii) post processing.

Properties and Characterization of Nickel Superalloy Powders

It is well known that powder characteristics such as particle size and shape distribution, chemical composition, and thermal conductivity have significant effects on the process efficiencies and the

quality of the final products (Figure 2) [10,11]. Olakanmi reported linear correlation between the powder packing and sintered density in SLS processed Al [12]. While Kong et al. reported best deposition efficiency for particle size range 60 – 80 microns in direct metal laser deposition of IN625 [13], Karapakis et al. suggested bimodal size distribution spherical particles for optimal packing condition [14]. Cleary and Sawley modeled powder discharge from hoppers and investigated the influence of powder aspect ratio on the mass flow rates [15]. Their results suggested a decrease in the flow rate as the shape changes from an equiaxed to an elongated form. Other than powder particle size and morphology, the thermal conductivity and chemical composition of powder materials also play an important role in defining the microstructural evolution and printability. Alkahari et al. [16] reported that the ability of powder materials to conduct heat which affects the consolidation process during additive manufacturing. It was also found in this study that the thermal conductivity of powder metals was influenced by the bulk density and particle size/morphology. The detrimental effects of impurities such as phosphorous, sulfur, carbon, and oxygen are also widely reported in the open literature [17].

For the above reasons, it became standard practice to characterize the feedstock powders for properties such as particle size distribution, morphology, density, and chemical composition as per ASTM F3049-14. Table 1 lists the particle size details of Ni superalloys used in different commercial and custom-built AM machines as obtained from the literature. The evaluation methods for particle size and morphology include sieving (ASTM B214-15), light scattering (ASTM B822-10) and other non-standardized methods such as image analysis. For density measurements, gas pycnometry (ASTM B923-10) and flow meters (ASTM B212-13, B417-13, B329-14, and B527-15) can be used. The chemical composition of Ni superalloy powders used in AM can be evaluated in accordance with ASTM E1473. Figure 3 shows the typical morphology and particle size distribution of nickel-based super alloy powder used in AM.

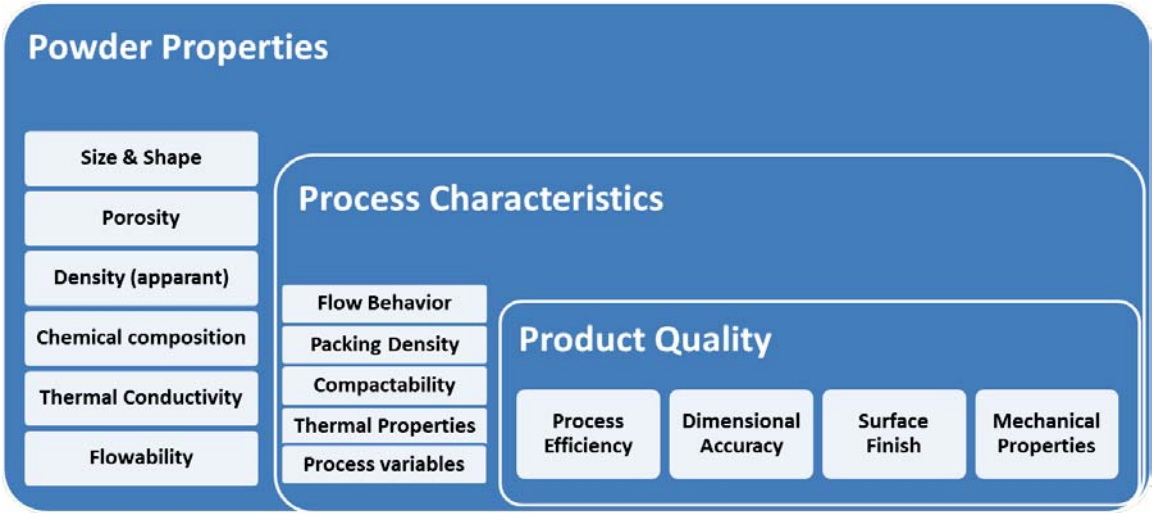

Figure 2 Influence of powder properties on process characteristics and build part quality

Table 1 Details of Ni super alloy powders used in different AM process

Material	Supplier	Particle Size (µm)	AM System	Reference
CM247LC	LPW Tech. Ltd.	15-70	SLM	[18,19]

CMSX-4®	Cannon Muskegeon Group	45-105	ARCAM	[20]
	Praxair Surface Technologies	20-150	SLE	[21–23]
Haynes 230	LPW Tech. Ltd.	15-45	Concept Laser	[24]
IC221W	Oak Ridge National Laboratory	45-105	LENS	[25]
IN100	Pratt & Whitney—HMI Metal Powders	20-150	SLE	[26]
	Sulzer Metco	20-45	Micro-LAAM	[27]
IN625	AP&C-Arcam	44-120	ARCAM	[28]
	LPW Tech. Ltd.	15-45	Concept Laser	[29]
	EOS	5-45	EOS	[30–32]
	Sandwik Osprey Ltd.	10-20	Phenix	[33,34]
	Praxript Inc.	45–135	Direct Metal Deposition	[35]
	Sulzer Metco	45-95	Trumpf Laser Depostion	[36]
	Micro-Melt ®	Different size ranges between 20 and 177		[13]
	H.C. Starck GmbH	20-150	HRPM-II machine Huazhong University of Science and Technology, China	[37]
IN718	EOS	5-45	EOS	[38–41]
	LPW Tech. Ltd.	5-50	Realizer	[42,43]
	N.A	<50	Self-developed SLM machine (LSNF-I)	[44]
IN738	Nanoval	6 - 41	Concept Laser	[45,46]
	N.A	45-135		[47]
	Erasteel	20 - 55	SLM	[48,49]
MAR M-509	LPW Tech. Ltd.	13-49	Concept Laser	[45]
MAR-M247	IKTS	D_{50} - 47	HT - SLM	[47]
René 41	GE	APS 72	LMD	[50,51]
René 80	Pratt & Whitney—HMI Metal Powders	20-150	SLE	[52]
René 142	GE	30 - 110	EBM	[53]
Waspaloy®	Special Metals	APS 63	SLM	[54]

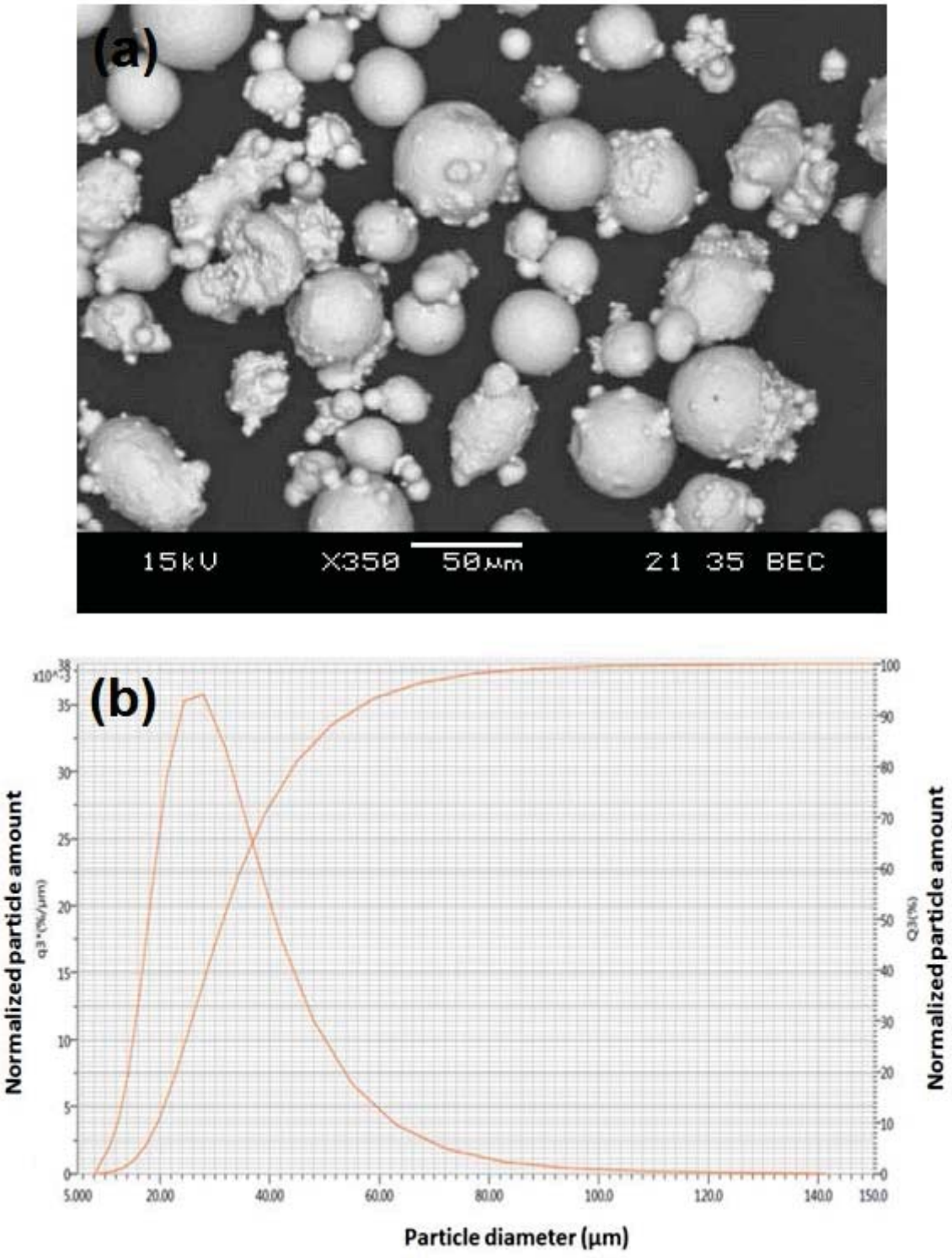

Figure 3 Representative images showing (a) the morphology and (b) particle size distribution of Ni superalloy powders used in AM process

In addition, the flow properties of powder raw materials are measured using Hall flowmeter (ASTM B213-13), Carney funnels (ASTM B964-09) and Arnold meter (ASTM B855-11) for a better understanding of powder packing and deposition. Available literature suggests that the flow characteristics of Ni superalloy powders depend on variables such as moisture content, particle size and distribution, particle shape, particle density and chemical composition [55]. While it is known that a higher degree of powder packing and good dispersion condition can yield dense parts, it is a challenge to determine theoretically the flow behavior of bulk solids with parameters such as particle morphology, distribution, inter-particle forces, moisture and temperature. This makes it difficult to clearly predict the process-ability of any new material. Krantz et al. [56] provided a comprehensive description of different techniques and suggested that results provided by each method are strongly dependent upon the powder stress condition. This indicates that no single technique is suitable for the full characterization of a powder and in principle, they complement each other.

The dynamic flow properties of powders can also be measured using new state-of-art technologies such as FT4 Powder Rheometer® and The Revolution Powder Analyzer®. Detailed procedure for using the Freeman Technology FT4 powder rheometer shear cell for shear testing of powders can be obtained from ASTM D7891–15. Similarly, the Revolution Powder Analyser can be used to quantify the powder's particle behavior during process applications (such as blending, tableting, mixing and transportation) by measuring the ability of powder to flow, consolidate, granulate, cake, pack and fluidize and correlating with the power, time and variances in energy of the powder in a rotating drum.

Influence of Processing & Post Processing Variables

In addition to the inherent flow and thermal characteristics of powder raw materials, process variables and post-processing conditions also control the printability of AM parts. Table 2 lists the mechanical properties of additively manufactured nickel superalloys. It shows that different AM technologies/printing strategies/processing variables/post-processing conditions produce parts with varying properties. The following are some of the parameters which are known to strongly influence the properties of AM parts.

Influence of built direction

With regards to microstructural development, it is generally perceived that the grain growth occurs from the cooler side to the warmer side. Since AM process involves layer-by-layer manufacturing approach, the successive stages of rapid heat conduction from the molten zone and the faster solidification facilitate columnar grain growth by rapid nucleation and growth along the direction of thermal gradient. Therefore, the samples built with a different building direction would have elongated grains along a different direction resulting in anisotropic properties (as shown in Table 2). Figure 4a shows the representative microstructural characteristics of a Ni superalloy captured along different direction (build direction represented by arrow). Further, it is also worth noting that the microstructural grains, dendrites and precipitates of the built parts are an order of magnitude smaller than that of the substrate material. Bansal et al. [23] observed a sharp change in the dendrite size of CMSX-4® superalloy (~15 times smaller dendrites in the built parts when compared to the similar substrate material processed by investment casting) fabricated using a custom built powder bed laser system (Figure 4b).

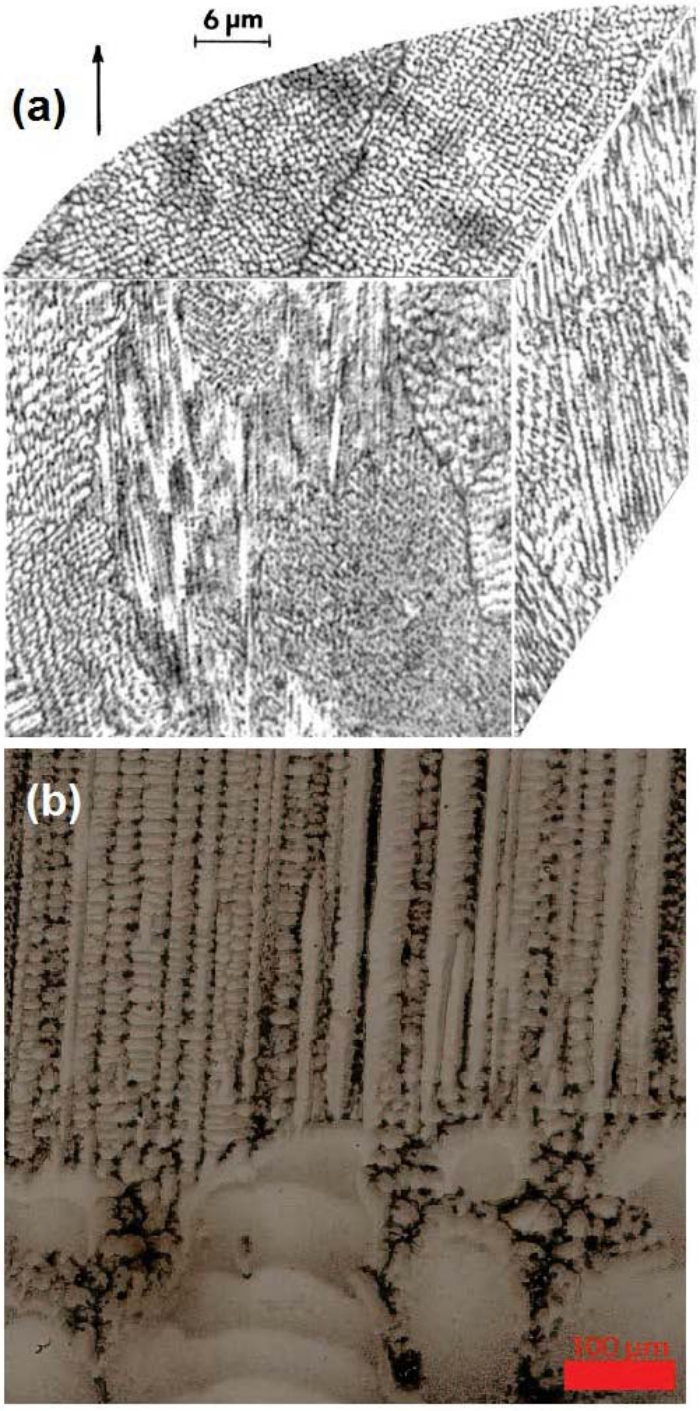

Figure 4 Micrographs showing (a) representative microstructure of SLM processed Inconel superalloy (directly adapted from [39]**), (b) Coarse to fine grain transition from substrate to deposit in CMSX-4® (adopted from Bansal et al.** [23]**)**

Table 2 Mechanical properties of additively manufactured nickel based super alloys

Materials	AM System	Youngs Modulus (GPa)		Yield Strength (MPa)		Ultimate Strength (MPa)		Elongation to failure (%)		References
		Build direction	Transverse Direction	Build direction	Transverse direction	Build direction	Transverse direction	Build direction	Transverse direction	
Haynes 230	Concept Laser	152±1	205±4	656±4	798±5	941±2	1102±6	32±3	28±1	[24]
IN625		159±5	200±3	579±5	734±3	888 ± 6	1036 ± 3	40±1	36±0.3	[29]
	EOS M290	140	170	615	725	900	990	42	35	[30]
	Phenix PM100	141±9	204±4	720±30	800±20	1070±60	1030±50	8-10		[34]
	Custom Built LRM	-		571±15		915±20		46-49		[57]
IN625 (HT)		-		395±15		824±25		48-54		
IN718	Realiser SLM250	162±18	193±24	572±44	643±63	904±22	991±62	19±4	13±6	[43]
	EOS M270	-	-	830		1120		25		[39]
	EOS M290	-	-	1034	1068	1309	1344	27	27	[38]
	SLM	-	-	737	816	1010	1085	20.6	19.1	[58]
	SMD	-	-	-	473	-	828	-	28	[59]
	DLD	-	-	650	1000	-	-	-	-	[60]

Table 2 Mechanical properties of additively manufactured nickel based super alloys (continued)

Materials	AM System	Youngs Modulus (GPa)		Yield Strength (MPa)		Ultimate Strength (MPa)		Elongation to failure (%)		References
		Build direction	Transverse Direction	Build direction	Transverse direction	Build direction	Transverse direction	Build direction	Transverse direction	
	EBF[3]	-	-	-	580	-	910	-	22	[6]
	Laser/Wire	-	-	-	1079	-	1314	-	20.4	
	Custom Built SLM	204		889-907		1137–1148		19.2-25.9		[44]
IN718 (HT)		201		1102-1161		1280–1358		10-22		
	EOS M270	-		880	930	1140	1200	30	27	[39]
	EOS M270	-		850	890	1140	1200	28	28	
	Realiser SLM250	163±30	199±15	1074±42	1159±32	1320±76	1377±66	19±2	8±6	[43]
	SLM	-	-	1136	1227	1357	1447	13.6	10.1	[58]
	DLD	-	-	1257	1436	-	-	-	-	[60]
		-	-	-	1098	-	1321	-	9.8	[61]
		-	-	-	1034	-	1276	-	12	[62]
	Laser/Wire	-	-	-	1079	-	1314	-	20.4	[63]

Influence of laser power and scanning speed

The degree of sintering and melting of powder particles to produce solid parts normally depends on the energy transferred to the powder which is influenced by the laser power, the scan speed and scan spacing. Gu and Shen [64] demonstrated different scanning strategies and reported that an optimal amount of laser power and scanning speed are required for the complete melting of powder particles (316L stainless steel) as shown in Figure 5.

Bauer et al. [24] investigated the effects of laser power, scan speed, layer thickness and hatch distance on the microstructural properties of Haynes 230 alloy. In this study, it was found that the mean grain size of AM parts decreases with the decrease in energy density, i.e. the mean grain size decrease with lower energy input. Similarly, the grain orientation tends to become random for faster scan rate (Figure 6). A comparison of key parameters used in different powder based AM process is shown in Table 3.

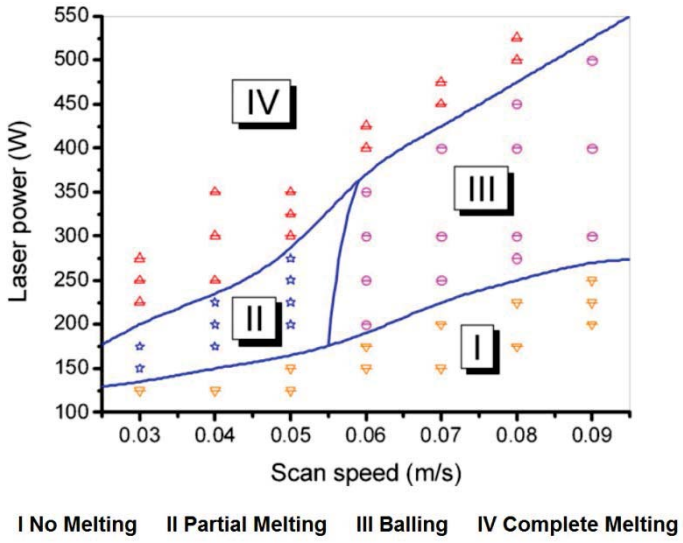

Figure 5 Effects of laser power and scan speed on degree of powder melting as depicted by different zones (directly adapted from Gu and Shen [64]**)**

Figure 6 IPF maps for Haynes® 230® using (a) 116 J/mm^3, (b) 77 J/mm^3 and (c) 66 J/mm^3 (directly adapted from Bauer et al. [24]**)**

Table 3 Comparison of key parameters used in AM process

Process	Technology	Layer Thickness (µm)	Laser Power (W)	Deposition Rate (cm^3/min)
Direct Metal Laser Sintering (DMLS)	Sintering	20-100	50-400	Depends on spot size, scan speed and size, number, and part complexity
Selective Laser Melting (SLS)	Melting	20-100	50-200	
Direct Laser Deposition (DLD)	Deposition	254	150-2000	0.1-4.1
Laser Engineered Net Shaping (LENS)	Deposition	130-380		-
Laser Rapid Forming (LRF)	Deposition	200		1

Influence of the hatch angle

Hatch angle can be defined as the angle between laser scanning directions on consecutive layers. It is important to note that the improper selection of hatch angle induces mechanical anisotropy in the built parts and hence, it has to be selected properly. Guan et al. [65] investigated the influence of hatch angle on the properties of 304 stainless steel. Samples prepared with hatch angles ranging from 90° - 150° were tested and the relationship between the number of layers, interval number, hatch angle and the properties were established. In this study, more satisfactory results were achieved for a hatch angle of 105°. It was also found that the mechanical isotropy improves with the growth of interval number. However, Paul et al. [57] suggested that this may not be true always as in the case of Inconel 625 wherein, the tensile properties were not much influenced by the hatch angle.

Guan et al. [65] suggested that the parameters such as layer thickness, overlap rate will not significantly affect the default properties of AM materials, provided other key variables are unaltered.

Influence of heat treatment

Since AM processes involve rapid solidification, residual stresses are often induced in the printed products and post processing heat treatment becomes essential to relive the induced residual stresses, which if not treated would detrimentally affect the product life. Furthermore, the heat treatment process can also be used to selectively modify the microstructure of built parts for desired performance requirements. The following heat treatment methods are generally recommended used for heat treating nickel based superalloys produced by AM processes.

1. Solution heat treatment (at 980 °C for 1hrs followed by air cooling) followed by homogenization and double aging (at 720 °C for 8hrs, followed by furnace cooling at 55°C/h to 620 °C, then kept for 8hrs and subsequently air cooled) for IN718
2. Solution heat treatment (at 982 °C for 0.5 h) and then hot isostatic pressing (at 1163 °C and 0.1 GPa for 4 h)
3. Annealing (at 1150 °C for 1 hour and followed by rapid cooling) for IN625

Conclusions

Based on the literature review, the following conclusions can be drawn regarding the additive manufacturing of nickel based superalloys.

1. Powder based methods such as SLS, SLM, EBM techniques based on partial and full melting of powder materials and powder deposition techniques can be successfully employed for additive manufacturing nickel based superalloys.
2. Powder properties such as particle size and shape distribution, chemical composition, thermal conductivity, etc. affects the properties of nickel superalloys processed using AM methods.
3. The final properties of Ni superalloys produced using AM methods also depend on the processing and post processing parameters.
4. The monotonous mechanical properties displayed by additively manufactured Ni superalloys are superior/similar to that of the conventionally processed materials

Bibliography

1. Gibson, I.; Rosen, D. W.; Stucker, B. Additive Manufacturing Technologies. *Addit. Manuf. Technol.* **2010**, 17–40.
2. LaMonica, M. Additive Manufacturing. *Technol. Rev.* **2013**, *116*, 58–59.
3. Gu, D. D.; Meiners, W.; Wissenbach, K.; Poprawe, R. Laser additive manufacturing of metallic components: materials, processes and mechanisms. *Int. Mater. Rev.* **2012**, *57*, 133–164.
4. Williams, C. B.; Mistree, F.; Rosen, D. W. Towards the design of a layer-based additive manufacturing process for the realization of metal parts of designed mesostructure. *Proc. 16th Solid Free. Fabr. Symp.* **2005**, 217–230.
5. Ding, D.; Pan, Z.; Cuiuri, D.; Li, H. Wire-feed additive manufacturing of metal components: technologies, developments and future interests. *Int. J. Adv. Manuf. Technol.* 2015, *81*, 465–481.
6. Bird, R. K.; Hibberd, J. Tensile Properties and Microstructure of Inconel 718 Fabricated with Electron Beam Freeform Fabrication (EBF 3). *Nasa/Tm-2009-215929* **2009**.
7. Wohlers, T. *Wohlers Report 2014. 3D Printing and Additive Manufacturing State of the Industry*; 2014.
8. Lewandowski, J. J.; Seifi, M. Metal Additive Manufacturing: A Review of Mechanical Properties. *Annu. Rev. Mater. Res* **2016**, *46*, 11–14.
9. Slotwinski, J.; Cooke, A.; Moylan, S. Mechanical properties testing for metal parts made via additive manufacturing: A review of the state of the art of mechanical property testing. In *Additive Manufacturing Materials: Standards, Testing and Applicability*; 2015; pp. 1–20.
10. Benson, J. M.; Snyders, E. The need for powder characterisation in the additive manufacturing. *South African J. Ind. Eng.* **2015**, *26*, 104–114.
11. Strondl, A.; Lyckfeldt, O.; Brodin, H.; Ackelid, U. Characterization and Control of Powder Properties for Additive Manufacturing. *JOM* **2015**, *67*, 549–554.
12. Olakanmi, E. O. Effect of mixing time on the bed density, and microstructure of selective laser sintered (SLS) aluminium powders. *Mater. Res.* **2012**, *15*, 167–176.
13. Kong, C. Y.; Carroll, P. A.; Brown, P.; Scudamore, R. J. The effect of average powder particle size on deposition efficiency, deposit height and surface roughness in the direct metal laser deposition process. In *14th International Conference on Joining of Materials*; 2007.
14. Karapatis, N. P.; Egger, G.; Gygax, P. E.; Glardon, R. Optimization of powder layer density in selective laser sintering. In *Proc. of Solid Freeform Fabrication Symposium 1999*; 1999; pp. 255–263.
15. Cleary, P. W.; Sawley, M. L. DEM modelling of industrial granular flows: 3D case studies and the effect of particle shape on hopper discharge. *Appl. Math. Model.* **2002**, *26*, 89–111.
16. Alkahari, M. R.; Furumoto, T.; Ueda, T.; Hosokawa, A.; Tanaka, R.; Aziz, A.; Sanusi, M. Thermal conductivity of metal powder and consolidated material fabricated via selective laser melting. In *Key Engineering Materials*; Trans Tech Publ, 2012; Vol. 523, pp. 244–249.
17. Xie, X.; Liu, X.; Hu, Y.; Tang, B.; Xu, Z.; Dong, J.; Ni, K.; Zhu, Y.; Tien, S.; Zhang, L. The role of phosphorus and sulfur in Inconel 718. *Superalloys 1996* **1996**, 599.
18. Divya, V. D.; Muñoz-Moreno, R.; Messé, O. M. D. M.; Barnard, J. S.; Baker, S.; Illston, T.; Stone, H. J. Microstructure of selective laser melted CM247LC nickel-based superalloy and its evolution through heat treatment. *Mater. Charact.* **2016**, *114*, 62–74.

19. Muñoz-Moreno, R.; Divya, V. D.; Driver, S. L.; Messé, O. M. D. .; Illston, T.; Baker, S.; Carpenter, M. A.; Stone, H. J. Effect of heat treatment on the microstructure, texture and elastic anisotropy of the nickel-based superalloy CM247LC processed by selective laser melting. *Mater. Sci. Eng. A* **2016**, *674*, 529–539.
20. Ramsperger, M.; Singer, R. F.; Körner, C. Microstructure of the Nickel-Base Superalloy CMSX-4 Fabricated by Selective Electron Beam Melting. *Metall. Mater. Trans. A Phys. Metall. Mater. Sci.* **2016**, *47*, 1469–1480.
21. Acharya, R.; Bansal, R.; Gambone, J. J.; Das, S. A microstructure evolution model for the processing of single-crystal alloy CMSX-4 through scanning laser epitaxy for turbine engine hot-section component repair (part II). *Metall. Mater. Trans. B* **2014**, *45*, 2279–2290.
22. Basak, A.; Acharya, R.; Das, S. Additive Manufacturing of Single-Crystal Superalloy CMSX-4 Through Scanning Laser Epitaxy: Computational Modeling, Experimental Process Development, and Process Parameter Optimization. *Metall. Mater. Trans. A* **2016**, *47*, 3845–3859.
23. Bansal, R.; Acharya, R.; Gambone, J. J.; Das, S. Experimental and Theoretical Analysis of Scanning Laser Epitaxy Applied to Nickel-based Superalloys. In *Solid Freeform Fabrication Symposium*; 2011; pp. 496–503.
24. Bauer, T; Dawson, K; Spierings, S.B; Wegener, K. Microstructure and mechanical characterisation of SLM processed Haynes 230. In *International Solid Free Form Fabrication Symposium*; Austin, Texax, USA, 2015; pp. 813–822.
25. Liu, W.; DuPont, J. N. Direct laser deposition of a single-crystal Ni_3Al-based IC221W alloy. *Metall. Mater. Trans. A* **2005**, *36*, 3397–3406.
26. Acharya, R.; Das, S. Additive Manufacturing of IN100 Superalloy Through Scanning Laser Epitaxy for Turbine Engine Hot-Section Component Repair: Process Development, Modeling, Microstructural Characterization, and Process Control. *Metall. Mater. Trans. A Phys. Metall. Mater. Sci.* **2015**.
27. Bi, G.; Sun, C. N.; Chen, H. Chi; Ng, F. L.; Ma, C. C. K. Microstructure and tensile properties of superalloy IN100 fabricated by micro-laser aided additive manufacturing. *Mater. Des.* **2014**, *60*, 401–408.
28. List, F. A.; Dehoff, R. R.; Lowe, L. E.; Sames, W. J. Properties of Inconel 625 mesh structures grown by electron beam additive manufacturing. *Mater. Sci. Eng. A* **2014**, *615*, 191–197.
29. Spierings, A. B.; Bauer, T; Dawson, K; Colella, A; Wegener, K. Processing ODS Modified IN625 using Selective Laser Melting. In *International Solid Free Form Fabrication Symposium*; Austin, Texax, USA, 2015; pp. 803–812.
30. Poyraz, Ö; Yasa, E; Akbulut, G; Orhangü, A; Pilatin. S. Investigation of support structures for direct metal laser sintering (DMLS) of IN625 parts. In *Internation Solid Free Form Fabrication Symposium*; Austin, Texax, USA, 2015; pp. 560–574.
31. Sateesh, N. H.; Kumar, G. C. M.; Prasad, K.; C.K., S.; Vinod, A. R. Microstructure and Mechanical Characterization of Laser Sintered Inconel-625 Superalloy. *Procedia Mater. Sci.* **2014**, *5*, 772–779.
32. Cooper, D. E.; Blundell, N.; Maggs, S.; Gibbons, G. J. Additive layer manufacture of Inconel 625 metal matrix composites, reinforcement material Investigation of support structures for direct metal laser sintering (DMLS) of IN625 parts evaluation. *J. Mater. Process. Technol.* **2013**, *213*, 2191–2200.
33. Yadroitsev, I.; Pavlov, M.; Bertrand, P.; Smurov, I. Mechanical properties of samples fabricated by selective laser melting. *14èmes Assises Eur. du Prototypage Fabr. Rapide*

2009, *625*, 24–25.
34. Yadroitsev, I.; Thivillon, L.; Bertrand, P.; Smurov, I. Strategy of manufacturing components with designed internal structure by selective laser melting of metallic powder. *Appl. Surf. Sci.* **2007**, *254*, 980–983.
35. Dinda, G. P.; Dasgupta, A. K.; Mazumder, J. Laser aided direct metal deposition of Inconel 625 superalloy: Microstructural evolution and thermal stability. *Mater. Sci. Eng. A* **2009**, *509*, 98–104.
36. Hong, C.; Gu, D.; Dai, D.; Alkhayat, M.; Urban, W.; Yuan, P.; Cao, S.; Gasser, A.; Weisheit, A.; Kelbassa, I.; Zhong, M.; Poprawe, R. Laser additive manufacturing of ultrafine TiC particle reinforced Inconel 625 based composite parts: Tailored microstructures and enhanced performance. *Mater. Sci. Eng. A* **2015**, *635*, 118–128.
37. Li, S.; Wei, Q.; Shi, Y.; Zhu, Z.; Zhang, D. Microstructure Characteristics of Inconel 625 Superalloy Manufactured by Selective Laser Melting. *J. Mater. Sci. Technol.* **2015**, *31*, 946–952.
38. Scott-Emuakpor, O.; Schwartz, J.; George, T.; Holycross, C.; Cross, C.; Slater, J. Bending fatigue life characterisation of direct metal laser sintering nickel alloy 718. *Fatigue Fract. Eng. Mater. Struct.* **2015**, *38*, 1105–1117.
39. Amato, K. N.; Gaytan, S. M.; Murr, L. E.; Martinez, E.; Shindo, P. W.; Hernandez, J.; Collins, S.; Medina, F. Microstructures and mechanical behavior of Inconel 718 fabricated by selective laser melting. *Acta Mater.* **2012**, *60*, 2229–2239.
40. Zhang, D.; Niu, W.; Cao, X.; Liu, Z. Materials Science & Engineering A Effect of standard heat treatment on the microstructure and mechanical properties of selective laser melting manufactured Inconel. *Mater. Sci. Eng. A* **2015**, *644*, 32–40.
41. Sanz, C.; García Navas, V. Structural integrity of direct metal laser sintered parts subjected to thermal and finishing treatments. *J. Mater. Process. Technol.* **2013**, *213*, 2126–2136.
42. Ardila, L. C.; Garciandia, F.; Gonz??lez-D??az, J. B.; ??lvarez, P.; Echeverria, A.; Petite, M. M.; Deffley, R.; Ochoa, J. Effect of IN718 recycled powder reuse on properties of parts manufactured by means of Selective Laser Melting. *Phys. Procedia* **2014**, *56*, 99–107.
43. Chlebus, E.; Gruber, K.; Kuźnicka, B.; Kurzac, J.; Kurzynowski, T. Effect of heat treatment on microstructure and mechanical properties of Inconel 718 processed by selective laser melting. *Mater. Sci. Eng. A* **2015**, *639*, 647–655.
44. Wang, Z.; Guan, K.; Gao, M.; Li, X.; Chen, X.; Zeng, X. The microstructure and mechanical properties of deposited-IN718 by selective laser melting. *J. Alloys Compd.* **2012**, *513*, 518–523.
45. Cloots, M.; Kunze, K.; Uggowitzer, P. J.; Wegener, K. Microstructural characteristics of the nickel-based alloy IN738LC and the cobalt-based alloy Mar-M509 produced by selective laser melting. *Mater. Sci. Eng. A* **2016**, *658*, 68–76.
46. Kunze, K.; Etter, T.; Gr??sslin, J.; Shklover, V. Texture, anisotropy in microstructure and mechanical properties of IN738LC alloy processed by selective laser melting (SLM). *Mater. Sci. Eng. A* **2014**, *620*, 213–222.
47. Engeli, R.; Etter, T.; H??vel, S.; Wegener, K. Processability of different IN738LC powder batches by selective laser melting. *J. Mater. Process. Technol.* **2016**, *229*, 484–491.
48. Geiger, F.; Kunze, K.; Etter, T. Tailoring the texture of IN738LC processed by selective laser melting (SLM) by specific scanning strategies. *Mater. Sci. Eng. A* **2016**, *661*, 240–246.
49. Rickenbacher, L.; Etter, T.; Hövel, S.; Wegener, K. High temperature material properties of IN738LC processed by selective laser melting (SLM) technology. *Rapid Prototyp. J.* **2013**, *19*, 282–290.

50. Li, J.; Wang, H. M.; Tang, H. B. Effect of heat treatment on microstructure and mechanical properties of laser melting deposited Ni-base superalloy Rene′41. *Mater. Sci. Eng. A* **2012**, *550*, 97–102.
51. Li, J.; Wang, H. M. Microstructure and mechanical properties of rapid directionally solidified Ni-base superalloy Rene'41 by laser melting deposition manufacturing. *Mater. Sci. Eng. A* **2010**, *527*, 4823–4829.
52. Acharya, R.; Bansal, R.; Gambone, J. J.; Kaplan, M. A.; Fuchs, G. E.; Rudawski, N. G.; Das, S. Additive Manufacturing and Characterization of René 80 Superalloy Processed Through Scanning Laser Epitaxy for Turbine Engine Hot-Section Component Repair. *Adv. Eng. Mater.* **2015**, *17*, 942–950.
53. Murr, L. E.; Martinez, E.; Pan, X. M.; Gaytan, S. M.; Castro, J. A.; Terrazas, C. A.; Medina, F.; Wicker, R. B.; Abbott, D. H. Microstructures of Rene 142 nickel-based superalloy fabricated by electron beam melting. *Acta Mater.* **2013**, *61*, 4289–4296.
54. Mumtaz, K. A.; Erasenthiran, P.; Hopkinson, N. High density selective laser melting of Waspaloy. *J. Mater. Process. Technol.* **2008**, *195*, 77–87.
55. Amado, a; Schmid, M.; Levy, G.; Wegener, K. Advances in SLS powder characterization. *22nd Annu. Int. Solid Free. Fabr. Symp. - An Addit. Manuf. Conf. SFF 2011, August 8, 2011 - August 10, 2011* **2011**, *12*, 438–452.
56. Krantz, M.; Zhang, H.; Zhu, J. Characterization of powder flow: Static and dynamic testing. *Powder Technol.* **2009**, *194*, 239–245.
57. Paul, C. P.; Ganesh, P.; Mishra, S. K.; Bhargava, P.; Negi, J.; Nath, A. K. Investigating laser rapid manufacturing for Inconel-625 components. *Opt. Laser Technol.* **2007**, *39*, 800–805.
58. Strößner, J.; Terock, M.; Glatzel, U. Mechanical and Microstructural Investigation of Nickel-Based Superalloy IN718 Manufactured by Selective Laser Melting (SLM). *Adv. Eng. Mater.* **2015**, n/a–n/a.
59. Baufeld, B. Mechanical properties of INCONEL 718 parts manufactured by shaped metal deposition (SMD). *J. Mater. Eng. Perform.* **2012**, *21*, 1416–1421.
60. Blackwell, P. L. The mechanical and microstructural characteristics of laser-deposited IN718. *J. Mater. Process. Technol.* **2005**, *170*, 240–246.
61. Zhang, Y.-N.; Cao, X.; Wanjara, P.; Medraj, M. Tensile properties of laser additive manufactured Inconel 718 using filler wire. *J. Mater. Res.* **2014**, *29*, 2006–2020.
62. Qi, H.; Azer, M.; Ritter, A. Studies of standard heat treatment effects on microstructure and mechanical properties of laser net shape manufactured INCONEL 718. *Metall. Mater. Trans. A Phys. Metall. Mater. Sci.* **2009**, *40*, 2410–2422.
63. Cao, X.; Rivaux, B.; Jahazi, M.; Cuddy, J.; Birur, A. Effect of pre-and post-weld heat treatment on metallurgical and tensile properties of Inconel 718 alloy butt joints welded using 4 kW Nd: YAG laser. *J. Mater. Sci.* **2009**, *44*, 4557–4571.
64. Gu, D.; Shen, Y. Processing conditions and microstructural features of porous 316L stainless steel components by DMLS. *Appl. Surf. Sci.* **2008**, *255*, 1880–1887.
65. Guan, K.; Wang, Z.; Gao, M.; Li, X.; Zeng, X. Effects of processing parameters on tensile properties of selective laser melted 304 stainless steel. *Mater. Des.* **2013**, *50*, 581–586.